

Exact mobility edges in quasiperiodic network models with slowly varying potentials

Hai-Tao Hu,^{1,2} Yang Chen,^{1,2} Xiaoshui Lin,^{1,2} Ai-Min Guo,³ Guangcan Guo,^{1,2} Ming Gong,^{1,2,*} and Zijing Lin^{1,2,†}

¹Department of Physics, University of Science and Technology of China, Hefei, Anhui 230026, China

²Hefei National Laboratory, University of Science and Technology of China, Hefei 230088, China

³Hunan Key Laboratory for Super-microstructure and Ultrafast Process, School of Physics, Central South University, Changsha 410083, China

(Dated: February 26, 2025)

Quasiperiodic potentials without self-duality are always hard to derive the exact mobility edges (MEs). Here, we propose a new class of network models with exactly solvable MEs, characterized by quasiperiodic slowly varying potentials that do not exhibit hidden self-duality. We present two methods to derive the MEs, the first involves integrating out the periodic sites to obtain an effective Hamiltonian with effective potential $g(E)V$ and effective eigenenergy $f(E)$, which directly yields the MEs at $f(E) = \pm(2t \pm g(E)V)$, and the second is to connect the localized-delocalized transition points of the quasiperiodic slowly varying models and the real-complex transition points of the eigenvalue equations. To illustrate this, we take quasiperiodic mosaic slowly varying models as examples, and we find that the MEs obtained from the two methods are the same. Furthermore, we generalize our methods to quasiperiodic network models and propose a possible experimental realization based on optical waveguide systems, showing that the Anderson transition can be observed even using small physical systems (with $L = 50 - 100$). Our results may provide insight into understanding and realizing exact MEs in experiments.

I. INTRODUCTION

The study of localization phenomena in low-dimensional systems has been one of the central problems in condensed matter physics [1–4]. In one-dimensional (1D) systems, the scaling theory of localization indicates that even extremely weak on-site random disorder leads to the localization of all eigenstates [5–10]. However, in models with correlated disorders, such as those involving quasiperiodic potentials [11–14], Anderson transitions occur at specific critical strengths. 1D models with quasiperiodic potentials can exhibit much rich physics, including localized, extended, and critical phases, along with the associated mobility edges (MEs) [15, 16]. A pedagogical example of such a quasiperiodic system is the Aubry-André-Harper (AAH) model [11, 17–22], in which the self-duality between real space and momentum space leads to the exact phase boundaries separating localized and extended states at the critical potential strength $V_c = \pm 2t$ [11]. Consequently, all states are extended when $|V| < |V_c|$, while they become localized for $|V| > |V_c|$, with states at the critical points exhibiting multifractality [23–25].

The concept of self-duality has been generalized to other quasiperiodic systems, including AAH chains with exponentially decaying hopping terms [26, 27], nearest-neighbor tight-binding chains with other quasiperiodic potentials [27–29], and quasiperiodic mosaic AAH models [30–35]. In these models, the MEs can be directly determined from self-duality. However, there also exists a much broader class of quasiperiodic systems lacking self-duality [36–44], whose MEs may also be exactly

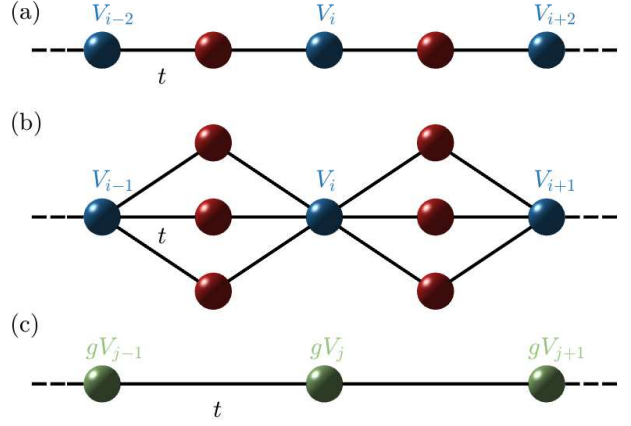


FIG. 1. (a) The 1D quasiperiodic mosaic model featuring a slowly varying incommensurate potential with $\kappa = 2$. (b) A special kind of quasiperiodic network model when $\gamma = 3$. This model can be interpreted as a multipath quasiperiodic model, where γ denotes the number of paths. (c) The effective quasiperiodic chain after integrating out periodic sites. Here, V_i represents the quasiperiodic slowly varying potential, expressed as $V \cos(\pi\alpha i^\nu + \phi)$, and gV_j is the effective potential.

solved using some other methods. For instance, several duality-breaking cases can be solved through the renormalization groups method [45, 46], and the quasiperiodic models with slowly varying potentials $V_i = V \cos(\pi\alpha i^\nu)$ can be exactly solved using semianalytical technique [47–51]. In particular, Das Sarma *et al.* demonstrated that 1D quasiperiodic models with slowly varying potentials $V_i = V \cos(\pi\alpha i^\nu)$ exhibit MEs at $E_c = \pm(2t - V)$ for $0 < \nu < 1$ and $V < 2$, while for $\nu > 1$, all states away from the exact band center are localized [49].

Recently, we demonstrated a method for determining

* gongm@ustc.edu.cn

† zjlin@ustc.edu.cn

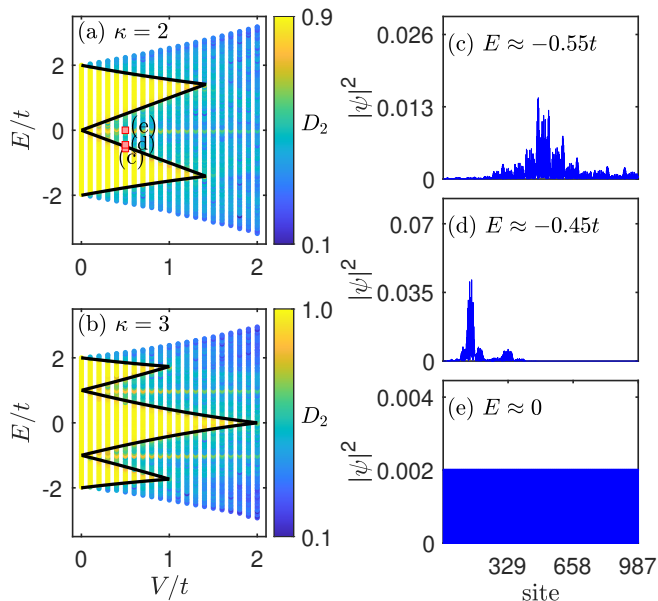


FIG. 2. Fractal dimension D_2 of different eigenstates as a function of energy E and potential strength V for quasiperiodic mosaic models with slowly varying potentials when (a) $\kappa = 2$ and (b) $\kappa = 3$. The solid lines denote the MEs given by Eqs. (3), (4), and (5), respectively. (c)-(e) Spatial distributions of three representative eigenstates with $E \approx -0.55t$ (extended), $E \approx -0.45t$ (localized), and $E = 0$ (resonant) as marked in Fig. 2(a). The other parameters are $\alpha = (\sqrt{5} - 1)/2$, $\nu = 0.6$, $\phi = 0$ and $L = 987$.

the MEs of various quasiperiodic network models with self-dual potentials, which is constituted by periodic network sites and quasiperiodic sites. We show that although the original models lack self-duality, the effective models obtained by integrating out the periodic sites exhibit hidden self-duality. Compared to the above models, quasiperiodic network models offer significantly greater flexibility, enabling us to design the MEs in much more physical models. The major idea of this work is to extend the discussion of MEs from network models with self-dual potentials to those with slowly varying potentials that lack self-duality. In this paper, we theoretically obtain the exact MEs for a new class of one-dimensional quasiperiodic network models with slowly varying potentials. Here, we present two methods to achieve this. The first involves integrating out the periodic sites to obtain an effective model with potential $g(E)V$ and energy $f(E)$, which directly yields the MEs at $f = \pm(2t \pm gV)$. It is worth mentioning that, in addition to the MEs separating extended states from localized states, the resonant states and the energy spectrum boundaries are also provided by the equation. The second method is to integrate out the periodic sites first and then follow the semi-analytical method proposed by previous work [49]. To validate our results, we take quasiperiodic mosaic models, the simplest case of quasiperiodic network models,

with slowly varying potentials as examples. We find that the MEs obtained by these two methods are the same. Finally, we illustrate this ideal with a special kind of quasiperiodic network model to obtain their exact MEs and provide a possible experimental realization.

The rest of the manuscript is organized as follows. Section II introduces the Hamiltonian of quasiperiodic mosaic models with slowly varying potentials and presents two methods to solve their MEs. Next, in Sec. III, we generalize our results to quasiperiodic network models with slowly varying potentials and consider a special type to obtain the MEs. In Sec. IV, we propose to realize these observations using optical waveguides. We demonstrate that the transition from extended phase to localized phase may be observed even with small physical systems ($L = 50 - 100$), which is currently realizable in experiments. Finally, we summarize our results in Sec. V.

II. MOSAIC MODELS WITH SLOWLY VARYING POTENTIALS

A. Hamiltonian and MEs

The quasiperiodic mosaic models with slowly varying potentials, as illustrated in Fig. 1(a), can be described by the Hamiltonian

$$\mathcal{H} = -t \sum_i (c_{i+1}^\dagger c_i + \text{H.c.}) + \sum_i V_i c_i^\dagger c_i. \quad (1)$$

Here, c_i^\dagger (c_i) represents the creation (annihilation) operator at site i , and t denotes the nearest-neighbor hopping coefficient. For simplicity, we set $t = 1$ as the energy unit. The on-site energy V_i follows a mosaic pattern and is defined as

$$V_i = \begin{cases} V \cos(\pi \alpha i^\nu + \phi), & \kappa |i| \\ 0, & \kappa \nmid i \end{cases}. \quad (2)$$

where κ is an integer, V denotes the on-site potential strength, and ϕ is the phase offset. Without loss of generality, we set $\phi = 0$ and $\alpha = (\sqrt{5} - 1)/2$, which can be approximated as $\lim_{n \rightarrow \infty} F_{n-1}/F_n$, where F_n are Fibonacci numbers defined by $F_{n+1} = F_n + F_{n-1}$ with $F_0 = F_1 = 1$. In this work, the system size L is taken as F_n and α is approximated by F_{n-1}/F_n .

When $\nu = 1$ and $\kappa = 1$, the model reduces to the well-known AAH model, which exhibits a phase transition between extended and localized states. Specifically, all states are extended for $|V| < 2t$ and localized for $|V| > 2t$, with $V = \pm 2t$ being the self-dual points where all states are critical [11]. For $\nu = 1$ and $\kappa \neq 1$, the model transitions to the quasiperiodic mosaic AAH model, where the hidden self-duality ensures the presence of MEs, such as $E_c = \pm 2t^2/V$ for the minimal case $\kappa = 2$, and $E_c = \pm \sqrt{t^2 \pm 2t^3/V}$ for $\kappa = 3$ [30]. When $0 < \nu < 1$ and $\kappa = 1$, the model corresponds to a quasiperiodic slowly varying model, where extended states are located

at the central region of the band ($|E| < 2t - V$) and localized states appear at the band edge ($|E| > 2t - V$). For $\nu > 1$ and $\kappa = 1$, all states away from the exact band center are localized [49].

In this work we focus on the condition that $0 < \nu < 1$ and $\kappa \neq 1$. One of the central results of this study is that the MEs in this model can be determined from the effective Hamiltonian, obtained by integrating out the periodic sites. For the minimal case of $\kappa = 2$, there are four exact energy-dependent MEs given by

$$E_c = \pm V, \quad E_c = \pm \frac{\sqrt{V^2 + 16t^2} - V}{2}, \quad (3)$$

with a maximum potential strength of $V_{\max} = \sqrt{2}t$. Additionally, there exists a resonant state at $E = 0$, where the wave function occupies only the sites with potential $V_i = 0$. Similarly, we can also obtain the MEs for $\kappa = 3$, which are given by

$$E_c = \pm \frac{V + t - \sqrt{V^2 - 2Vt + 9t^2}}{2}, \quad (4)$$

and

$$E_c = \pm \frac{V - t \pm \sqrt{V^2 + 2Vt + 9t^2}}{2}, \quad (5)$$

with $V_{\max} = 2t$ for $E = 0$ and $V_{\max} = t$ for $E = \pm\sqrt{3}t$. In this case, two resonant states exist at $E = \pm t$. In the following, we first present the numerical results in Sec. II B and then present the detailed derivations of these results in Sec. II C and Sec. II D.

B. Numerical results

We can characterize the localization properties of the wave functions by calculating the inverse participation ratio (IPR). For a normalized wave function $|\psi^n\rangle = \sum_i u_i^n c_i^\dagger |0\rangle$, the IPR is defined as

$$\text{IPR}^n = \sum_{i=1}^L |u_i^n|^4, \quad (6)$$

where n represents the band index. For an extended eigenstate, the IPR scales inversely with the chain length, $\text{IPR}^n \propto L^{-1}$, which approaches zero in the thermodynamic limit. Conversely, for a localized state, the IPR maintains a finite value as the system size increases, $\text{IPR}^n \propto L^0$. For a critical state, the IPR scales as $\text{IPR}^n \propto L^{-D_2}$, where the fractal dimension $D_2 \in (0, 1)$. To distinguish the extended, localized, and critical states, we can define the fractal dimension as

$$D_2^n = - \lim_{L \rightarrow \infty} [\ln \text{IPR}^n / \ln L]. \quad (7)$$

Figure 2(a) plots the fractal dimension of the corresponding eigenstates as a function of the energy and

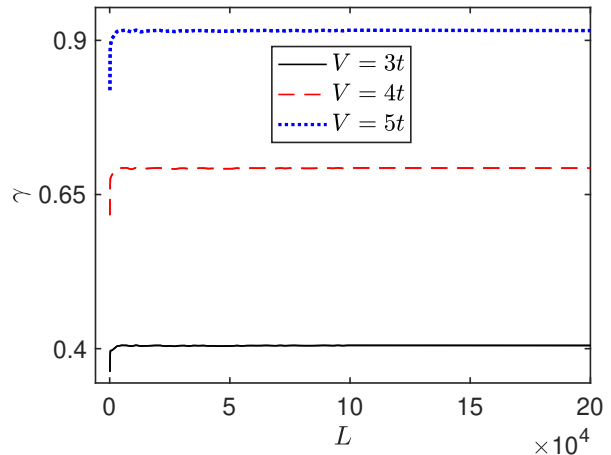


FIG. 3. Lyapunov exponent γ as a function of chain length L for quasiperiodic slowly varying model at various potential strength V when $E = 0$. The Lyapunov exponent gradually converges as the chain length increases.

potential strength for $\kappa = 2$. The black lines in the figure represent the MEs given by Eq. (3). Consistent with the analytical results, the fractal dimension D_2 is approximately one for energies satisfying $V < |E| < (\sqrt{V^2 + 16t^2} - V)/2$ and zero for other energies. For any κ , the model exhibits 2κ MEs, similar to the mosaic AAH model [30]. The validity of the MEs is further confirmed by the spatial distributions of three typical eigenstates, marked by pink squares in Fig. 2(a). Figures 2(c)-2(e) display the spatial distribution of these eigenstates, corresponding to $E \approx -0.55t$ (extended), $-0.45t$ (localized), and 0 (resonant) when $V = 0.5t$, respectively. These results are consistent with Eq. (3), which predicts extended states for $0.5t < |E| < 1.76556t$. Additionally, we plot the fractal dimension of the corresponding eigenstates for $\kappa = 3$ in Fig. 2(b), which fits well with the MEs given by Eqs. (4) and (5).

The above analysis can give invaluable information about the localization properties of the wave functions. For the localized states, we expect that the wave functions follow

$$|\psi(x)| \sim e^{-\gamma(x-x_0)}. \quad (8)$$

Here, $\gamma = \gamma(E)$, termed as Lyapunov exponent, depends on the energy E , and x_0 is the center position of state. Furthermore, we use the transfer matrix method to determine the Lyapunov exponent, which is the inverse localization length. Specifically, when the tight-binding model involves only nearest-neighbor hopping terms, i.e.,

$$-\psi_{i-1} - \psi_{i+1} + V_i \psi_i = E \psi_i, \quad (9)$$

it can be transformed into the following form

$$\begin{pmatrix} \psi_{i+1} \\ \psi_i \end{pmatrix} = T_i \begin{pmatrix} \psi_i \\ \psi_{i-1} \end{pmatrix}, \quad (10)$$

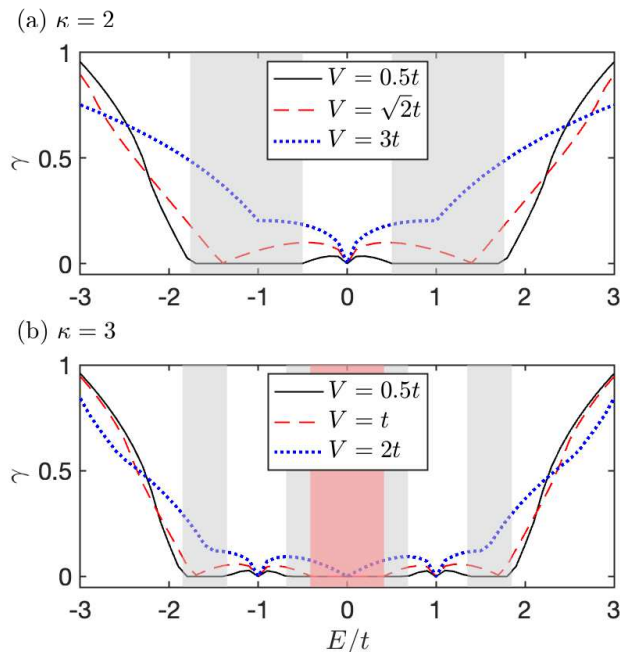


FIG. 4. Lyapunov exponent γ as a function of energy E for quasiperiodic mosaic models with slowly varying potentials at various V when (a) $\kappa = 2$ and (b) $\kappa = 3$. When the energy satisfies the conditions of Eqs. (3), (4), and (5), γ transitions from zero to a finite value, indicating the existence of MEs. The system size is $L = 832040$, and the other parameters are the same with those in Fig. 2.

where the transfer matrix T_i is defined as

$$T_i = \begin{pmatrix} V_i - E & -1 \\ 1 & 0 \end{pmatrix}. \quad (11)$$

Then we can define a new matrix

$$\mathbf{\Lambda} = \lim_{L \rightarrow \infty} (\mathbf{T}_L^\dagger \mathbf{T}_L)^{1/(2L)}, \quad \mathbf{T}_L = \prod_{i=1}^N T_i. \quad (12)$$

The Lyapunov exponents γ are then obtained as

$$\gamma(E) = \min_i (\ln \Lambda_i), \quad (13)$$

where Λ_i represents the eigenvalues of the matrix $\mathbf{\Lambda}$. In this case, the smallest Lyapunov exponent corresponds to the condition with longest localization length by definition $\gamma = 1/\xi$. Therefore, for the localized we expect γ is finite; while for the extended phase, we should have $\gamma L > 1$ (or $\gg 1$), where L is the chain length. We solve this matrix using the QR decomposition method. In Fig. 3, we plot the Lyapunov exponent γ versus L of the quasiperiodic slowly varying model for various V when $E = 0$, showing that this value is divergent. This results may indicate of ergodicity, which is necessary during the calculation of the above expression.

To further investigate the localization properties of the quasiperiodic mosaic model with slowly varying potentials in the thermodynamic limit, we plot the Lyapunov

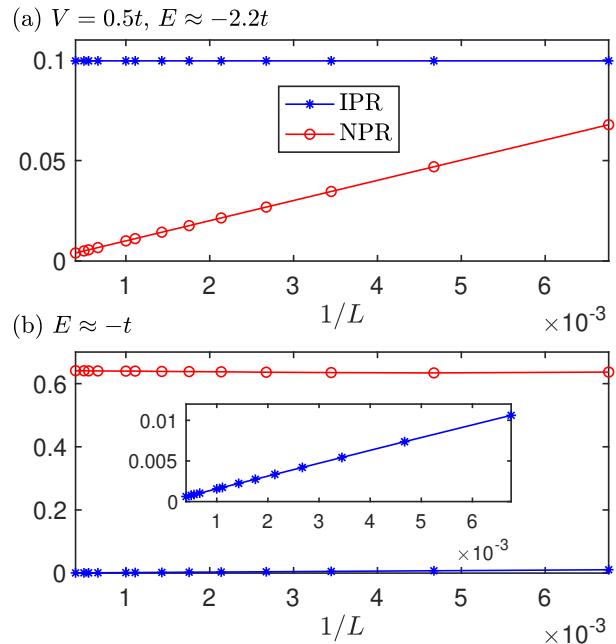


FIG. 5. Finite-size scaling of the IPR (blue asterisk) and NPR (red round) when $V = 0.5t$ for (a) localized state $E \approx -2.2t$ and (b) extended state $E \approx -t$. The inset in (b) provides an enlarged view of the scaling of IPR for the extended state. The other parameters are the same with those in Fig. 2.

exponent γ as a function of energy E for various V in Fig. 4. As the energy varies, γ changes dramatically from a finite value (indicating of localized states) to 0 (indicating of extended states), or vice versa, at certain energies. This abrupt jumping in γ suggests the presence of MEs in the energy spectrum. When $\kappa = 2$, we observe that the Lyapunov exponent at the exact band center is vanishing small ($\ll 1/L$) for different values of V [see Fig. 4(a)], indicating a resonant state. The MEs are clearly observed around $E_c \approx \pm 1.8t$ and $\pm 0.5t$ for $V = 0.5t$, and around $E_c \approx \pm 1.4t$ for $V = \sqrt{2}t$, which closely align with the exact expression of MEs given by Eq. (3). When $\kappa = 3$, we can also find the Lyapunov exponent γ for states satisfying $E = \pm t$ is always zero, indicating two resonant states [see Fig. 4(b)]. Additionally, the area of $\gamma = 0$ is consistent with the Eq. (4) and Eq. (5).

In Fig. 5, we show the scaling behavior of the IPR and NPR for (a) the localized state $E \approx -2.2t$, and (b) the extended state $E \approx -t$ when $\kappa = 2$ and $V = 0.5t$. For the extended state, the NPR is independent of the system size, and the IPR decreases to zero following the law of L^{-1} , with $D_2 \rightarrow 1$, corresponding to an extended state. For the localized state, when $L \rightarrow \infty$, the NPR decreases to zero as L^{-1} and the IPR remains constant. These results further demonstrate the existence of localization-delocalization transition in the model.

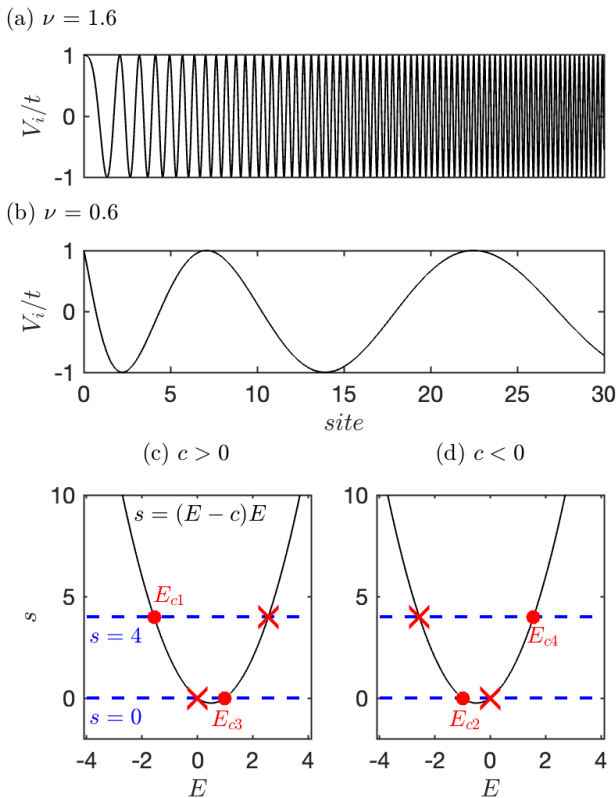


FIG. 6. Function $\cos(\pi\alpha j^\nu)$ with (a) $\nu = 1.6$ and (b) $\nu = 0.6$. (c) and (d) show $s = (E - c)E$ with $c > 0$ and $c < 0$, respectively, and their corresponding regime for $0 < s < 4$. The red dots denote the MEs.

with effective potential and effective eigenenergy

$$\lambda_j = EV \cos(2^\nu \pi \alpha j^\nu + \phi), \quad f(E) = E^2 - 2t^2. \quad (25)$$

The effective potential λ_j exhibits the property of becoming locally constant in the thermodynamic limit

$$\lim_{j \rightarrow \infty} \left| \frac{d\lambda_j}{dj} \right| = \lim_{j \rightarrow \infty} -EV 2^\nu \pi \alpha \nu \frac{\sin(2^\nu \pi \alpha j^\nu + \phi)}{j^{1-\nu}} = 0, \quad (26)$$

due to $0 < \nu < 1$ [see Fig. 6(b)]. When $\nu > 1$, the oscillating of the potential will become more rapid, yielding fully localized states in the thermodynamic limit [see Fig. 6(a)].

For the eigenstates of slowly varying models, one always expect its wave function with amplitude

$$u_j \sim z^j, \quad (27)$$

where z is a complex quantity, thus $|z| = 1$. The effective eigenvalue equation then becomes

$$t^2 z^{j-1} + [(E - V_j)E - 2t^2]z^j + t^2 z^{j+1} = 0, \quad (28)$$

with

$$V_j = V \cos(2^\nu \pi \alpha j^\nu + \phi), \quad (29)$$

which satisfies $|V_j| \leq V$. The crucial point is that when V_j is locally constant for large j , in the vicinity of this regime we can treat it to be a constant, that is,

$$V_j \approx c \text{ locally independent of } j \text{ for large } j, \quad (30)$$

with $-V \leq c \leq V$, yielding the following simplified solution

$$t^2 z^2 + [(E - c)E - 2t^2]z + t^2 = 0, \quad (31)$$

with the discriminant given by

$$\Delta = [(E - c)E]^2 - 4t^2[(E - c)E], \quad (32)$$

and

$$z = \frac{1}{2t^2}(-E^2 + cE + 2t^2 \pm \sqrt{\Delta}). \quad (33)$$

Based on this equation, Das Sarma *et al.* [49] pointed out that the real-complex transition points of the above eigenvalue equation are the extended-localized transition points of the quasiperiodic model. If $\Delta < 0$, the amplitude z is complex, satisfying $|z| = 1$, which means that the state is extended. Then we can conclude that the conditions for extended states are

$$0 < (E - c)E < 4t^2. \quad (34)$$

For $E > 0$, the conditions become

$$\begin{aligned} [(E - c)E]_{\max} &= [(E + V)E] < 4t^2, \\ [(E - c)E]_{\min} &= [(E - V)E] > 0 \Rightarrow E > V, \end{aligned} \quad (35)$$

while for $E < 0$, they become

$$\begin{aligned} [(E - c)E]_{\max} &= [(E - V)E] < 4t^2, \\ [(E - c)E]_{\min} &= [(E + V)E] > 0 \Rightarrow E < -V. \end{aligned} \quad (36)$$

Combining Eqs. (35) and (36), the exact MEs are determined by Eq. (3) [see Figs. 6(c) and 6(d)].

III. NETWORK MODELS WITH SLOWLY VARYING POTENTIALS

A. Hermitian models

The method of solving the MEs in quasiperiodic mosaic models with slowly varying potentials through effective Hamiltonian can be generalized to various quasiperiodic network models with slowly varying potentials [35]. Consider a concrete case that can be described by the Hamiltonian

$$\begin{aligned} \mathcal{H} &= \sum_{i=1}^L (V_i c_i^\dagger c_i + \sum_{k=1}^{\gamma} U_k d_{i,k}^\dagger d_{i,k}) - t \left(\sum_{i=1}^L \sum_{k=1}^{\gamma} c_i^\dagger d_{i,k} \right. \\ &\quad \left. + \sum_{i=1}^{L-1} \sum_{k=1}^{\gamma} c_{i+1}^\dagger d_{i,k} + \text{H.c.} \right), \end{aligned} \quad (37)$$

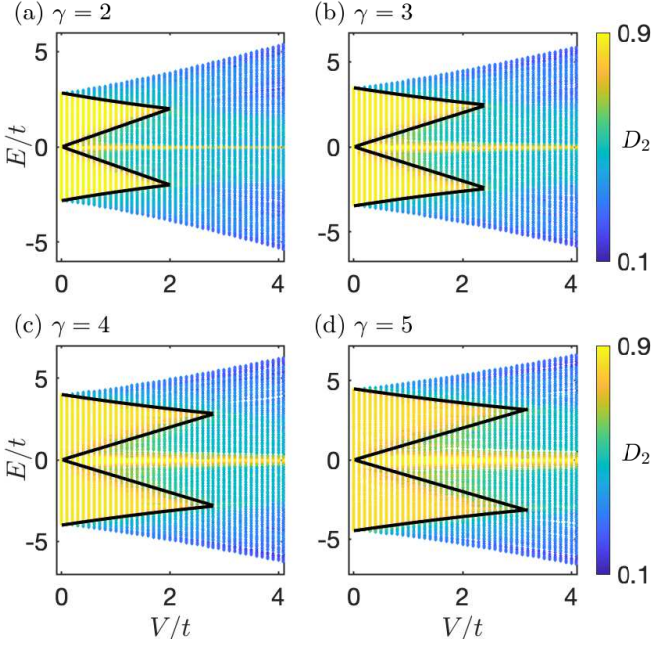


FIG. 7. Fractal dimension D_2 of different eigenstates as a function of energy E and potential strength V for multipath quasiperiodic chain with slowly varying potentials when (a) $\gamma = 2$, (b) $\gamma = 3$, (c) $\gamma = 4$, and (d) $\gamma = 5$. The solid lines denote the MEs described by $f(E) = \pm(2t \pm g(E)V)$ with function $f(E)$ and $g(E)$ given in Eq. (41). The other parameters are the same with Fig. 2.

where $d_{i,k}^\dagger$ ($d_{i,k}$) is the creation (annihilation) operator at the k -th site of cell i , V_i denotes the quasiperiodic slowly varying potentials defined as $V_i = V \cos(\pi\alpha i^\nu)$, and U_k represents constant potentials. Here we set $U_k = 0$ for simplicity, and the results for nonzero cases are similar. Figure 2(b) illustrates the multipath quasiperiodic network model with $\gamma = 3$. For such a multipath quasiperiodic model, the MEs can also be obtained through the effective Hamiltonian. To see that, we begin with the eigenvalue equations for the periodic sites

$$v_{i-1,k} = \frac{-tu_{i-1} - tu_i}{E}, \quad v_{i,k} = \frac{-tu_i - tu_{i+1}}{E}, \quad (38)$$

where $|\psi^n\rangle = \sum_i (u_i^n c_i^\dagger + \sum_k v_{i,k}^n d_{i,k}^\dagger) |0\rangle$. Substituting these into the eigenvalue equation for u_i yields

$$(E - V_i)u_i = \frac{t^2\gamma(u_{i-1} + 2u_i + u_{i+1})}{E}, \quad (39)$$

Rewrite u_i as u_j to distinguish between the effective chain and original chain, we obtain the effective Hamiltonian

$$\sum_j g(E)V \cos(\pi\alpha j^\nu)u_j + t^2u_{j-1} + t^2u_{j+1} = f(E)u_j, \quad (40)$$

with

$$g(E) = \frac{E}{\gamma}, \quad f(E) = -2t^2 + \frac{E^2}{\gamma}, \quad (41)$$

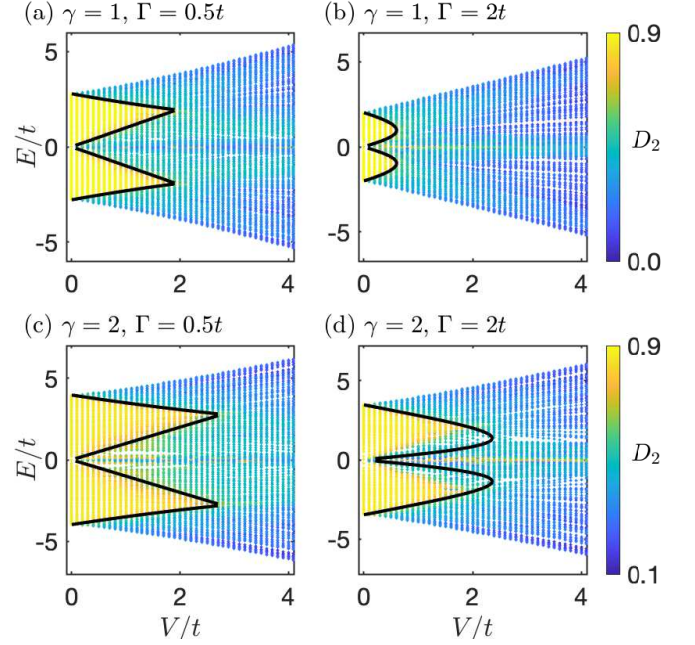


FIG. 8. Fractal dimension D_2 of different eigenstates as a function of energy E and potential strength V for PT-symmetric multipath quasiperiodic chain with slowly varying potentials when (a) $\gamma = 1, \Gamma = 0.5t$, (b) $\gamma = 1, \Gamma = 2t$, (c) $\gamma = 2, \Gamma = 0.5t$, and (d) $\gamma = 2, \Gamma = 2t$. The solid lines denote the MEs described by $f(E) = \pm(2t \pm g(E)V)$ with function $f(E)$ and $g(E)$ given in Eq. (46). The other parameters are the same with Fig. 2.

which leads to the MEs at $f(E) = \pm(2t \pm g(E)V)$.

In Fig. 7, the fractal dimension of the eigenstates is plotted as a function of energy and potential strength for various γ . The black lines represent the MEs described by $f(E) = \pm(2t \pm g(E)V)$, with the corresponding $f(E)$ and $g(E)$ given in Eq. (41). It is observed that the value of γ doesn't affect the number of MEs, which remains fixed at 4 for various γ , in contrast to the influence of κ . Additionally, there always exists a state at $E = 0$, i.e., resonant state, which remains extended regardless of V .

B. Non-Hermitian models

The results for the non-Hermitian quasiperiodic network models with slowly varying potentials can be obtained in the same way. Here, we consider a special case with parity-time (PT) symmetry, which can be described as

$$\mathcal{H} = \sum_{i=1}^L (V_i c_i^\dagger c_i + \sum_{k=1}^{\gamma} i\Gamma d_{i,2k}^\dagger d_{i,2k} - i\Gamma d_{i,2k-1}^\dagger d_{i,2k-1}) - t \left(\sum_{i=1}^L \sum_{k'=1}^{2\gamma} c_i^\dagger d_{i,k'} + \sum_{i=1}^{L-1} \sum_{k'=1}^{2\gamma} c_{i+1}^\dagger d_{i,k'} + \text{H.c.} \right). \quad (42)$$

The PT symmetry is realized by balanced gain and loss in the periodic sites. The eigenvalue equations for the periodic sites are

$$v_{i,2k} = \frac{-tu_i - tu_{i+1}}{E - i\Gamma}, \quad v_{i,2k-1} = \frac{-tu_i - tu_{i+1}}{E + i\Gamma}, \quad (43)$$

Substituting these equations into the eigenvalue equation for u_i , we obtain

$$(E - V_i)u_i = \frac{2\gamma Et^2(u_{i-1} + 2u_i + u_{i+1})}{E^2 + \Gamma^2}. \quad (44)$$

Rewrite u_i using u_j leads to the following effective Hamiltonian

$$\sum_j g(E)V \cos(\pi\alpha j^\nu)u_j + t^2u_{j-1} + t^2u_{j+1} = f(E)u_j, \quad (45)$$

with

$$g(E) = \frac{(E^2 + \Gamma^2)}{2\gamma E}, \quad f(E) = -2t^2 + \frac{E^2 + \Gamma^2}{2\gamma}. \quad (46)$$

This solution will yields MEs at $f(E) = \pm(2t \pm g(E)V)$, which is numerically verified in Fig. 8 for various γ and Γ . The results for the other non-Hermitian cases can be derived in the same way.

IV. EXPERIMENTAL PROPOSAL

The realization of quasiperiodic network models with various periodic network sites is challenging in cold-atom systems [52–54], thus we propose an experimental scheme based on coupled optical single-mode waveguides [17, 55–57]. By controlling the distance between neighboring waveguides and tuning their refraction index, we can modulate the hopping strength and on-site potential [58, 59], enabling the realization of various quasiperiodic network models with slowly varying potentials. To observe the localized-delocalized transition in such systems, we can inject light into a single waveguide and measure the distribution of light intensity after it has propagated through a certain distance in the waveguides array [see Fig. 9(a)]. The propagation of light along the waveguide can be described by tight-binding equation

$$i\partial_z\psi(i, z) = H\psi(i, z), \quad (47)$$

where $\psi(i, z)$ represents the wave function at i -th waveguide, z is the propagation axis of the light, and H is the Hamiltonian of the quasiperiodic network models with slowly varying potentials. For localized states, the output light tends to be localized in one of the waveguides, while for extended states, it tends to occupy the whole chain. By varying system parameters, such as the potential strength and hopping term, one can explore the transitions between localized and extended states.

In Fig. 9(b), we plot the fractal dimension of the eigenstates as a function of energy E and potential strength V for a small system ($L = 100$), where we can also see clear MEs. Here we consider quasiperiodic mosaic model with slowly varying potentials when $\kappa = 2$ as an example. To simulate the experimental results, we plot the evolution of the wavefunction for various potential strength V in Figs. 9(c)-9(f). Although the specific wavefunction evolution depends on the initial state, the properties of localized state or extended state remain the same. Here, we set the initial state as $\psi(i, 0) = |0, \dots, 1_{i=50}, \dots, 0\rangle$. For $V = 0.5t$, the wave function gradually spreads through the entire system. As the potential strength increases to $V = t$, the wavefunction propagating to the boundary decreases, since the number of extended states in the system is reduced. When $V = 2t$ and $V = 3t$, the wavefunctions become localized around the center of the system, as all states away from the band center are localized. These results provide some theoretical basis for future experiments.

Here, we only demonstrate the possible observation of localized-delocalized transition with the increasing of potential strength in network models in some small systems. The precise phase boundary from this kind of measurement can't be precisely determined in the current stage, which is a common problem in all quantum simulating systems [60–62]; see our discussion in the next section. New algorithm is required to address this difficulty, which will be explored in future.

V. CONCLUSIONS

We propose a new class of 1D quasiperiodic network models with exact MEs, which are featured by slowly varying potentials. Unlike the previously proposed quasiperiodic network models [35], this new class doesn't exhibit hidden self-duality, since the potential $\cos(\pi\alpha i^\nu)$ is not self-dual. To obtain the MEs of quasiperiodic network models with slowly varying potentials, we present two distinct methods. The first involves integrating out the periodic sites to obtain an effective model, where $g(E)V$ represents the effective potential and $f(E)$ denotes the effective eigenenergy. Substituting f and g into $f = \pm(2t \pm gV)$ gives the concrete MEs. It should be noted that $f = \pm(2t \pm gV)$ is not guaranteed by the hidden self-duality, but comes from the MEs of the original slowly varying models. Additionally, we present a more convinced method by connecting the real-complex transition points of the eigenvalue equations and the localized-delocalized transition points of the quasiperiodic chain, which yields results in excellent agreement with the results of the first method.

Now, it is quite possible that we are in a position to reflect on the possible future of quantum simulations. In this work, we show that the rich phases in the quasiperiodic network models can be simulated using some simulation platforms, including optical and acoustic waveguides

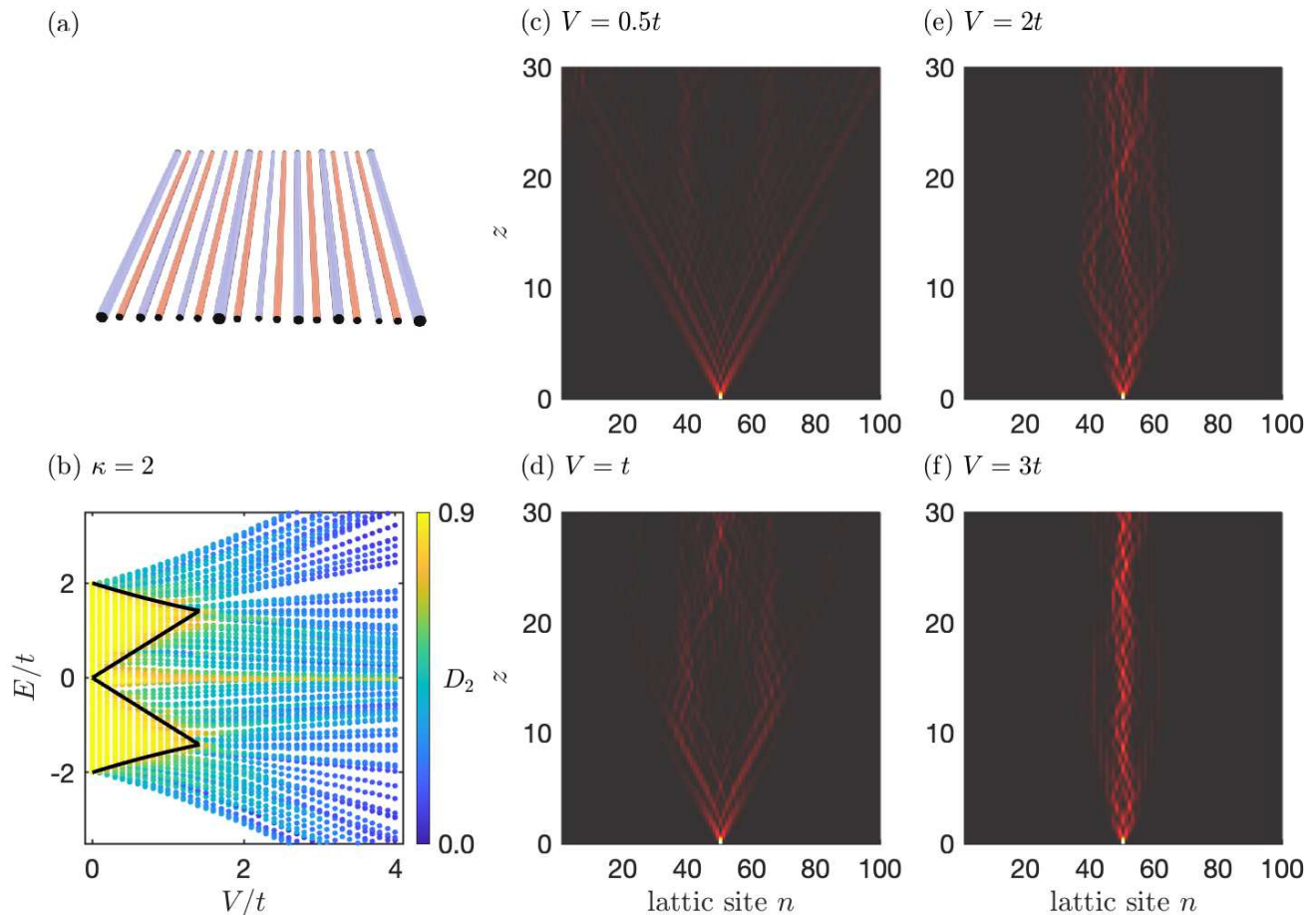


FIG. 9. (a) An illustration of the experimental setup based on a waveguide system for quasiperiodic mosaic model with $\kappa = 2$. Here, the blue waveguides have quasiperiodic slowly varying potentials, while the red ones have zero potential. (b) Fractal dimension D_2 of different eigenstates as a function of energy E and potential strength V for $L = 100$. The solid lines denote the MEs described by Eq. (3). Evolution of the wave function $\psi(i, z)$ for the initial state $\psi(i, 0) = \delta_{i,50}$ when (c) $V = 0.5t$, (d) $V = t$, (e) $V = 2t$, and (f) $V = 3t$.

[63–65], ultracold atoms, superconducting qubits [66–71], in which most of the important physics can be obtained using some small quantum systems. In recent years, these small systems have been used to demonstrate these fundamental physics. Yet, the detailed physics, including the scaling laws and the phase boundaries has not been determined. This is different from that in the community of condensed matter physics, in which the phase transition and the associated scaling exponents can be precisely determined in experiments. The similar accuracy has not yet been achieved in quantum simulation. In the future, with the increasing of experimental techniques, it is quite possible that these simulating platforms can be used to determine the precise phase boundary and the associated critical exponents, making quantum simulations a powerful tool to explore possible new physics. At the present stage, only some intriguing phenomena have been simulated. If this kind of accuracy has been achieved, the physical models may serve as an important platform for

exploring Anderson transition in the network models [72], which will help us to resolve the long-standing problems in this physics. Especially, in the presence of many-body interaction [73–75] and in the higher dimensional models with various potentials [76, 77], the physics cannot be efficiently simulated using classical computers, and these possible new physics may be simulated using these intriguing platforms.

ACKNOWLEDGMENTS

This work is supported by the National Natural Science Foundation of China (Grant No. 12374017, No. 12074362) and the Innovation Program for Quantum Science and Technology (2021ZD0303303, 2021ZD0301200, 2021ZD0301500). A.-M. G. is supported by the NSFC (Grant Nos. 12274466 and 11874428) and the Hunan Provincial Science Fund for Distinguished Young Schol-

-
- [1] T. Schwartz, G. Bartal, S. Fishman, and M. Segev, Transport and anderson localization in disordered two-dimensional photonic lattices, *Nature* **446**, 52 (2007).
- [2] G. Roati, C. D'Errico, L. Fallani, M. Fattori, C. Fort, M. Zaccanti, G. Modugno, M. Modugno, and I. M., Anderson localization of a non-interacting bose-einstein condensate, *Nature* **453**, 895 (2008).
- [3] J. Billy, V. Josse, Z. Zuo, A. Bernard, B. Hambrecht, P. Lugan, D. Clément, L. Sanchez-Palencia, P. Bouyer, and A. A., Direct observation of anderson localization of matter waves in a controlled disorder, *Nature* **453**, 891 (2008).
- [4] M. Segev, Y. Silberberg, and D. Christodoulides, Anderson localization of light, *Nat. Photon.* **7**, 197 (2013).
- [5] P. W. Anderson, Absence of diffusion in certain random lattices, *Phys. Rev.* **109**, 1492 (1958).
- [6] D. J. Thouless, Electrons in disordered systems and the theory of localization, *Phys. Rep.* **13**, 93 (1974).
- [7] E. Abrahams, P. W. Anderson, D. C. Licciardello, and T. V. Ramakrishnan, Scaling theory of localization: Absence of quantum diffusion in two dimensions, *Phys. Rev. Lett.* **42**, 673 (1979).
- [8] A. MacKinnon and B. Kramer, One-parameter scaling of localization length and conductance in disordered systems, *Phys. Rev. Lett.* **47**, 1546 (1981).
- [9] S. Sarker and E. Domany, Scaling theory of anderson localization: A renormalization-group approach, *Phys. Rev. B* **23**, 6018 (1981).
- [10] F. Evers and A. D. Mirlin, Anderson transitions, *Rev. Mod. Phys.* **80**, 1355 (2008).
- [11] S. Aubry and G. André, Analyticity breaking and anderson localization in incommensurate lattices, *Ann. Israel Phys. Soc.* **3**, 18 (1980).
- [12] P. G. Harper, Single band motion of conduction electrons in a uniform magnetic field, *Proceedings of the Physical Society. Section A* **68**, 874 (1955).
- [13] X. Li, S. Ganeshan, J. H. Pixley, and S. Das Sarma, Many-body localization and quantum nonergodicity in a model with a single-particle mobility edge, *Phys. Rev. Lett.* **115**, 186601 (2015).
- [14] R. Modak and S. Mukerjee, Many-body localization in the presence of a single-particle mobility edge, *Phys. Rev. Lett.* **115**, 230401 (2015).
- [15] V. Goblot, A. Štrkalj, N. Pernet, J. L. Lado, C. Dorow, A. Lemaitre, L. Le Gratiet, A. Harouri, I. Sagnes, S. Ravets, A. Amo, B. J., and Z. O., Emergence of criticality through a cascade of delocalization transitions in quasiperiodic chains, *Nat. Phys.* **16**, 832 (2020).
- [16] J. Gao, I. M. Khaymovich, X.-W. Wang, Z.-S. Xu, A. Iovan, G. Krishna, J. Jiensi, A. Cataldo, A. V. Balatsky, V. Zwiller, and A. W. Elshaari, Probing multi-mobility edges in quasiperiodic mosaic lattices, *Science Bulletin* <https://doi.org/10.1016/j.scib.2024.09.030> (2024).
- [17] Y. E. Kraus, Y. Lahini, Z. Ringel, M. Verbin, and O. Zeitler, Topological states and adiabatic pumping in quasicrystals, *Phys. Rev. Lett.* **109**, 106402 (2012).
- [18] X. Cai, L.-J. Lang, S. Chen, and Y. Wang, Topological superconductor to anderson localization transition in one-dimensional incommensurate lattices, *Phys. Rev. Lett.* **110**, 176403 (2013).
- [19] S. Ganeshan, K. Sun, and S. Das Sarma, Topological zero-energy modes in gapless commensurate aubry-andré-harper models, *Phys. Rev. Lett.* **110**, 180403 (2013).
- [20] J. Wang, X.-J. Liu, G. Xianlong, and H. Hu, Phase diagram of a non-abelian aubry-andré-harper model with p -wave superfluidity, *Phys. Rev. B* **93**, 104504 (2016).
- [21] S. Longhi, Topological phase transition in non-hermitian quasicrystals, *Phys. Rev. Lett.* **122**, 237601 (2019).
- [22] S. Roy, T. Mishra, B. Tanatar, and S. Basu, Reentrant localization transition in a quasiperiodic chain, *Phys. Rev. Lett.* **126**, 106803 (2021).
- [23] M. Wilkinson, Critical properties of electron eigenstates in incommensurate systems, *Proc. R. Soc. Lond. A* **391**, 305 (1984).
- [24] A. P. Siebesma and L. Pietronero, Multifractal properties of wave functions for one-dimensional systems with an incommensurate potential, *Europhysics Letters* **4**, 597 (1987).
- [25] C. Tang and M. Kohmoto, Global scaling properties of the spectrum for a quasiperiodic schrödinger equation, *Phys. Rev. B* **34**, 2041 (1986).
- [26] J. Biddle and S. Das Sarma, Predicted mobility edges in one-dimensional incommensurate optical lattices: An exactly solvable model of anderson localization, *Phys. Rev. Lett.* **104**, 070601 (2010).
- [27] T. Liu, H. Guo, Y. Pu, and S. Longhi, Generalized aubry-andré self-duality and mobility edges in non-hermitian quasiperiodic lattices, *Phys. Rev. B* **102**, 024205 (2020).
- [28] S. Ganeshan, J. H. Pixley, and S. Das Sarma, Nearest neighbor tight binding models with an exact mobility edge in one dimension, *Phys. Rev. Lett.* **114**, 146601 (2015).
- [29] Y. Wang, X. Xia, Y. Wang, Z. Zheng, and X.-J. Liu, Duality between two generalized aubry-andré models with exact mobility edges, *Phys. Rev. B* **103**, 174205 (2021).
- [30] Y. Wang, X. Xia, L. Zhang, H. Yao, S. Chen, J. You, Q. Zhou, and X.-J. Liu, One-dimensional quasiperiodic mosaic lattice with exact mobility edges, *Phys. Rev. Lett.* **125**, 196604 (2020).
- [31] Y. Liu, Y. Wang, X.-J. Liu, Q. Zhou, and S. Chen, Exact mobility edges, \mathcal{PT} -symmetry breaking, and skin effect in one-dimensional non-hermitian quasicrystals, *Phys. Rev. B* **103**, 014203 (2021).
- [32] Z.-H. Wang, F. Xu, L. Li, D.-H. Xu, and B. Wang, Topological superconductors and exact mobility edges in non-hermitian quasicrystals, *Phys. Rev. B* **105**, 024514 (2022).
- [33] X.-C. Zhou, Y. Wang, T.-F. J. Poon, Q. Zhou, and X.-J. Liu, Exact new mobility edges between critical and localized states, *Phys. Rev. Lett.* **131**, 176401 (2023).
- [34] Q. Dai, Z. Lu, and Z. Xu, Emergence of multifractality through cascadelike transitions in a mosaic interpolating aubry-andré-fibonacci chain, *Phys. Rev. B* **108**, 144207 (2023).
- [35] H.-T. Hu, X. Lin, A.-M. Guo, Z. Lin, and M. Gong,

- Hidden self-duality in quasiperiodic network models (2024), [arXiv:2411.06843 \[cond-mat.dis-nn\]](https://arxiv.org/abs/2411.06843).
- [36] J. Biddle, D. J. Priour, B. Wang, and S. Das Sarma, Localization in one-dimensional lattices with non-nearest-neighbor hopping: Generalized anderson and aubry-andré models, *Phys. Rev. B* **83**, 075105 (2011).
- [37] X. Deng, S. Ray, S. Sinha, G. V. Shlyapnikov, and L. Santos, One-dimensional quasicrystals with power-law hopping, *Phys. Rev. Lett.* **123**, 025301 (2019).
- [38] N. Roy and A. Sharma, Fraction of delocalized eigenstates in the long-range aubry-andré-harper model, *Phys. Rev. B* **103**, 075124 (2021).
- [39] J. Fraxanet, U. Bhattacharya, T. Grass, M. Lewenstein, and A. Dauphin, Localization and multifractal properties of the long-range kitaev chain in the presence of an aubry-andré-harper modulation, *Phys. Rev. B* **106**, 024204 (2022).
- [40] H. Yao, A. Khoudli, L. Bresque, and L. Sanchez-Palencia, Critical behavior and fractality in shallow one-dimensional quasiperiodic potentials, *Phys. Rev. Lett.* **123**, 070405 (2019).
- [41] X. Li and S. Das Sarma, Mobility edge and intermediate phase in one-dimensional incommensurate lattice potentials, *Phys. Rev. B* **101**, 064203 (2020).
- [42] X. Lin, X. Chen, G.-C. Guo, and M. Gong, General approach to the critical phase with coupled quasiperiodic chains, *Phys. Rev. B* **108**, 174206 (2023).
- [43] X. Lin and M. Gong, Fate of localization in a coupled free chain and a disordered chain, *Phys. Rev. A* **109**, 033310 (2024).
- [44] S.-Z. Li, Y.-C. Zhang, Y. Wang, S. Zhang, S.-L. Zhu, and Z. Li, Multifractal-enriched mobility edges and emergent quantum phases in a rydberg-dimer system, *Phys. Rev. Lett.* **134**, 055701 (2025), [arXiv:2501.07866 \[cond-mat.dis-nn\]](https://arxiv.org/abs/2501.07866).
- [45] M. Gonçalves, B. Amorim, E. V. Castro, and P. Ribeiro, Critical phase dualities in 1d exactly solvable quasiperiodic models, *Phys. Rev. Lett.* **131**, 186303 (2023).
- [46] M. Gonçalves, B. Amorim, E. V. Castro, and P. Ribeiro, Renormalization group theory of one-dimensional quasiperiodic lattice models with commensurate approximants, *Phys. Rev. B* **108**, L100201 (2023).
- [47] M. Griniasty and S. Fishman, Localization by pseudorandom potentials in one dimension, *Phys. Rev. Lett.* **60**, 1334 (1988).
- [48] D. J. Thouless, Localization by a potential with slowly varying period, *Phys. Rev. Lett.* **61**, 2141 (1988).
- [49] S. Das Sarma, S. He, and X. C. Xie, Mobility edge in a model one-dimensional potential, *Phys. Rev. Lett.* **61**, 2144 (1988).
- [50] S. Das Sarma, S. He, and X. C. Xie, Localization, mobility edges, and metal-insulator transition in a class of one-dimensional slowly varying deterministic potentials, *Phys. Rev. B* **41**, 5544 (1990).
- [51] T. Liu and H. Guo, Mobility edges in off-diagonal disordered tight-binding models, *Phys. Rev. B* **98**, 104201 (2018).
- [52] C. Gross and I. Bloch, Quantum simulations with ultracold atoms in optical lattices, *Science* **357**, 995 (2017), <https://www.science.org/doi/pdf/10.1126/science.aal3837>.
- [53] A. Browaeys and T. Lahaye, Many-body physics with individually controlled rydberg atoms, *Nat. Phys.* **16**, 132 (2020).
- [54] F. Schäfer, T. Fukuhara, and S. Sugawa, Tools for quantum simulation with ultracold atoms in optical lattices, *Nat. Rev. Phys.* **2**, 411 (2020).
- [55] D. Christodoulides, F. Lederer, and Y. Silberberg, Discretizing light behaviour in linear and nonlinear waveguide lattices, *Nature* **424**, 817 (2003).
- [56] Y. Lahini, R. Pugatch, F. Pozzi, M. Sorel, R. Morandotti, N. Davidson, and Y. Silberberg, Observation of a localization transition in quasiperiodic photonic lattices, *Phys. Rev. Lett.* **103**, 013901 (2009).
- [57] M. Verbin, O. Zilberberg, Y. E. Kraus, Y. Lahini, and Y. Silberberg, Observation of topological phase transitions in photonic quasicrystals, *Phys. Rev. Lett.* **110**, 076403 (2013).
- [58] A. Szameit, D. Blömer, J. Burghoff, T. Schreiber, T. Pertsch, S. Nolte, A. Tünnermann, and F. Lederer, Discrete nonlinear localization in femtosecond laser written waveguides in fused silica, *Opt. Express* **13**, 10552 (2005).
- [59] Y. Chen, X. Chen, X. Ren, M. Gong, and G.-c. Guo, Tight-binding model in optical waveguides: Design principle and transferability for simulation of complex photonics networks, *Phys. Rev. A* **104**, 023501 (2021).
- [60] I. M. Georgescu, S. Ashhab, and F. Nori, Quantum simulation, *Rev. Mod. Phys.* **86**, 153 (2014).
- [61] U. L. Heras, A. Mezzacapo, L. Lamata, S. Filipp, A. Wallraff, and E. Solano, Digital quantum simulation of spin systems in superconducting circuits, *Phys. Rev. Lett.* **112**, 200501 (2014).
- [62] E. Altman, K. R. Brown, G. Carleo, L. D. Carr, E. Demler, C. Chin, B. DeMarco, S. E. Economou, M. A. Eriksen, K.-M. C. Fu, M. Greiner, K. R. Hazzard, R. G. Hulet, A. J. Kollár, B. L. Lev, M. D. Lukin, R. Ma, X. Mi, S. Mitra, C. Monroe, K. Murch, Z. Nazario, K.-K. Ni, A. Ryb, D. T. S. Brown, M. Saffman, M. Schleier-Smith, I. Siddiqi, R. Simmonds, M. Singh, I. Spielman, K. Temme, D. S. Weiss, J. Vučković, V. Vuletić, J. Ye, and M. Zwierlein, Quantum simulators: Architectures and opportunities, *PRX Quantum* **2**, 017003 (2021).
- [63] A. Khelif, A. Choujaa, S. Benchabane, B. Djafari-Rouhani, and V. Laude, Guiding and bending of acoustic waves in highly confined phononic crystal waveguides, *Applied Physics Letters* **84**, 4400 (2004).
- [64] D. J. Apigo, W. Cheng, K. F. Dobiszewski, E. Prodan, and C. Prodan, Observation of topological edge modes in a quasiperiodic acoustic waveguide, *Phys. Rev. Lett.* **122**, 095501 (2019).
- [65] A. Coutant, A. Sivadon, L. Zheng, V. Achilleos, O. Richoux, G. Theocharis, and V. Pagneux, Acoustic su-schrieffer-heeger lattice: Direct mapping of acoustic waveguides to the su-schrieffer-heeger model, *Phys. Rev. B* **103**, 224309 (2021).
- [66] J. You and F. Nori, Atomic physics and quantum optics using superconducting circuits, *Nature* **474**, 589 (2011).
- [67] L. Jiang, C. L. Kane, and J. Preskill, Interface between topological and superconducting qubits, *Phys. Rev. Lett.* **106**, 130504 (2011).
- [68] R. C. Bialczak, M. Ansmann, M. Hofheinz, M. Lenander, E. Lucero, M. Neeley, A. D. O'Connell, D. Sank, H. Wang, M. Weides, J. Wenner, T. Yamamoto, A. N. Cleland, and J. M. Martinis, Fast tunable coupler for superconducting qubits, *Phys. Rev. Lett.* **106**, 060501 (2011).
- [69] E. Jeffrey, D. Sank, J. Y. Mutus, T. C. White, J. Kelly, R. Barends, Y. Chen, Z. Chen, B. Chiaro, A. Dunsworth, A. Megrant, P. J. J. O'Malley, C. Neill, P. Roushan,

- A. Vainsencher, J. Wenner, A. N. Cleland, and J. M. Martinis, Fast accurate state measurement with superconducting qubits, [Phys. Rev. Lett. **112**, 190504 \(2014\)](#).
- [70] C. Wang, Y. Gao, I. Pop, V. U., A. C., B. T., H. R., F. L., D. M., C. G., G. L., and S. R., Measurement and control of quasiparticle dynamics in a superconducting qubit, [Nat. Commun. **5**, 5836 \(2014\)](#).
- [71] V. Brosco, G. Serpico, V. Vinokur, N. Poccia, and U. Vool, Superconducting qubit based on twisted cuprate van der waals heterostructures, [Phys. Rev. Lett. **132**, 017003 \(2024\)](#).
- [72] P. Sierant, M. Lewenstein, and A. Scardicchio, Universality in Anderson localization on random graphs with varying connectivity, [SciPost Phys. **15**, 045 \(2023\)](#).
- [73] S. Iyer, V. Oganesyan, G. Refael, and D. A. Huse, Many-body localization in a quasiperiodic system, [Phys. Rev. B **87**, 134202 \(2013\)](#).
- [74] R. Vosk, D. A. Huse, and E. Altman, Theory of the many-body localization transition in one-dimensional systems, [Phys. Rev. X **5**, 031032 \(2015\)](#).
- [75] S. Bera, H. Schomerus, F. Heidrich-Meisner, and J. H. Bardarson, Many-body localization characterized from a one-particle perspective, [Phys. Rev. Lett. **115**, 046603 \(2015\)](#).
- [76] J. Argüello-Luengo, A. González-Tudela, T. Shi, P. Zoller, and J. I. Cirac, Quantum simulation of two-dimensional quantum chemistry in optical lattices, [Phys. Rev. Res. **2**, 042013 \(2020\)](#).
- [77] R. Ott, T. V. Zache, F. Jendrzejewski, and J. Berges, Scalable cold-atom quantum simulator for two-dimensional qed, [Phys. Rev. Lett. **127**, 130504 \(2021\)](#).